

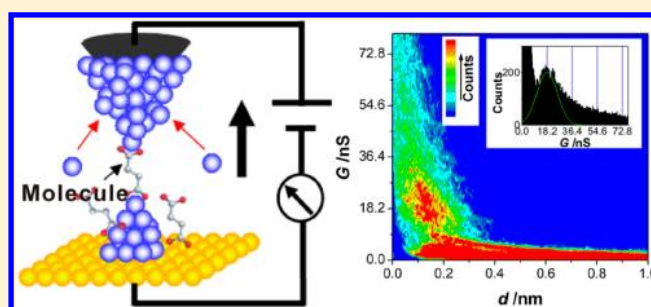
Single Molecule Conductance of Carboxylic Acids Contacting Ag and Cu Electrodes

Zheng-Lian Peng,[†] Zhao-Bin Chen,[‡] Xiao-Yi Zhou,[†] Yan-Yan Sun,[†] Jing-Hong Liang,[‡] Zheng-Jiang Niu,[†] Xiao-Shun Zhou,^{*,†} and Bing-Wei Mao^{*,‡}

[†]Key Laboratory of the Ministry of Education for Advanced Catalysis Materials, Institute of Physical Chemistry, Zhejiang Normal University, Jinhua, Zhejiang 321004, P. R. China

[‡]State Key Laboratory for Physical Chemistry of Solid Surfaces and Chemistry Department, College of Chemistry and Chemical Engineering, Xiamen University, Xiamen, Fujian 361005, P. R. China

ABSTRACT: In this work, the single molecule conductance of alkanedicarboxylic acid ($\text{HOOC}-(\text{CH}_2)_n-\text{COOH}$, $n = 1-5$) binding to Cu and Ag electrodes is systematically studied by using the electrochemical jump-to-contact scanning tunneling microscopy break junction approach (ECSTM-BJ). The results show that the conductance depends on molecular length and the electrode materials, which give a decay constant β_N of 0.95 ± 0.02 per $(-\text{CH}_2)$ unit for Cu electrodes and 0.71 ± 0.03 for Ag electrodes. The contact conductance shows the order of $G_{n=0,\text{Cu}} > G_{n=0,\text{Ag}}$. These differences can be attributed to the different electronic coupling efficiencies between molecules and electrodes. The conductance of ultrashort molecular junctions is also studied using oxalic acid as the target molecule, the results revealing that the through-space mechanism (TS) should be considered when the distance between two electrodes is very short. The present work demonstrates that electrode materials play an important role on the molecular conductance, contact conductance, and also the tunneling decay constant.



INTRODUCTION

Metal–molecule–metal junctions exhibiting electrical properties of amplification,^{1–5} rectification,^{6,7} and negative differential resistance,^{8–10} have received wide attention, which may be used in future molecular electronic devices.^{11–21} Many factors can influence the conductance of molecular junctions, such as the nature of molecular structure and the molecule–electrode contact.^{14,15,22–24} Typically, the latter includes contact geometry,^{25–28} anchoring groups,^{22,29–31} and electrode materials^{32–35} in the molecular junctions, which can cause not only the different electronic coupling efficiencies at the electrode–molecule contacts but also the energy level alignment between the molecular electronic level and Fermi level of the electrode,^{33,36} thus altering the conductance of molecular junctions. While a great number of the investigations are focused on the contact geometry and anchoring groups, there are few reports on the influence of electrode materials other than Au.^{25,33,37–39} In particular, systematic studies on the conductance measurements of homologous series of molecular junctions^{33,34,37} are limited. This restricts comprehensive understanding of electron transfer in molecular junction systems.

The electrochemical jump-to-contact scanning tunneling microscopy break junction approach (ECSTM-BJ) has been proven to form atomic-size nanowires of different metal electrodes^{40–42} for conductance measurements.⁴³ More recently, we demonstrated that ECSTM-BJ is suitable for

conductance measurement of single molecular junctions with different metallic electrodes.³⁶ The metal electrode can be easily changed by using different solutions containing target deposited metal. To the best of our knowledge, no systematic research is reported on the molecule length dependence of *single molecule conductance* contacting to Cu and Ag electrodes.

In this work, alkanedicarboxylic acid ($\text{HOOC}-(\text{CH}_2)_n-\text{COOH}$, $n = 1-5$) binding to the Cu and Ag electrodes is systematically investigated employing ECSTM-BJ, for the carboxylic acid can interact with those metals via the carboxylate group ($-\text{COO}^-$);^{44–46} then the different decay constants and contact conductances of Cu and Ag electrodes are discussed. In addition, the ultrashort molecule junctions with oxalic acid are measured, from which the electron transport mechanism can be derived by combining the long molecular junctions.

EXPERIMENTAL SECTION

Au(111) surfaces were obtained from single crystal beads without experiencing mechanical polishing, then used as the substrate, and mechanically cut Pt–Ir tips were used. The tips were insulated by thermosetting polyethylene glue to reduce the leakage current of electrochemical reaction. Platinum wire

Received: July 12, 2012

Revised: September 18, 2012

Published: September 19, 2012

was used as the counter electrode, while Cu and Ag wires were used as the reference electrodes for conductance measurements of Cu and Ag molecular junctions, respectively. $\text{HOOC}-(\text{CH}_2)_n-\text{COOH}$ ($n = 0-5$), Na_2SO_4 (99.9955%), CuSO_4 (99.999%), and Ag_2SO_4 (99.999%) were purchased from Alfa-Asia and used as received, and all aqueous solutions were prepared with ultrapure water ($>18 \text{ M}\Omega \text{ cm}$).

Conductance measurements were carried out on the modified Nanoscope IIIa STM (Veeco, US). The procedures for molecular conductance measurement were described previously.^{36,43} First, the metal is continuously electrodeposited onto the tip with STM feedback enabled (Figure 1a). Second,

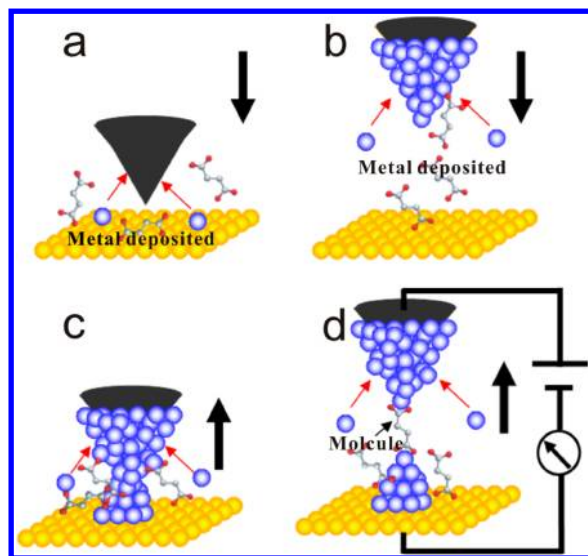


Figure 1. Schematic illustration of the ECSTM-BJ approach for conductance measurement of single molecular junctions with different metallic electrodes.

the deposited tip is pulled away from the Au(111) surface for about several tens of nanometers with the STM feedback disabled with negligibly small mechanical and thermal drift seen from the STM image in Figure 1b. Third, the tip is driven toward the surface until a given current (such as 8 nA) is reached. A jump-to-contact process, in that atoms of deposited metal on the tip transfer to the substrate and then form a metallic contact of the deposited metal, happens upon the application of a preset voltage pulse to the z -piezo of STM scanner which leads the tip toward the substrate. Then the tip is

pulled out of the contact at a typical speed such as 20 nm/s, to form atomic-size wire of the deposited metal (Figure 1c). Fourth, molecular junctions with deposited metal as electrodes are formed after breaking of the atomic-size metal wires. The current vs distance curve is recorded during the pulling of the tip at sampling frequency of 20 kHz. By repeating the whole process at new positions on the surface, well-controlled deposited metal contact can be realized. A large number (from hundreds to thousands) of conductance traces are collected to construct a conductance histogram. All experiments were made at a fixed bias voltage of 50 mV.

RESULTS AND DISCUSSION

Conductance of Malonic Acid Contacting with Cu and Ag Electrodes.

ECSTM-BJ was used to measure the single molecule conductance carried out in the aqueous solution containing 1 mM CuSO_4 + 1 mM malonic acid + 50 mM Na_2SO_4 . Pt-Ir tip and Au(111) were controlled at -5 mV and 45 mV vs Cu wire, respectively. Thus, metal bulk deposition on the tip can occur while bulk deposition on Au(111) is forbidden. Figure 2b is a typical conductance histogram of malonic acid ($\text{HOOC}-(\text{CH}_2)_n-\text{COOH}$, $n = 1$), which is constructed from hundreds of individual conductance traces as shown in Figure 2a. It shows preferential peak occurrence at 55 nS, corresponding to the conductance of Cu-(malonic acid)-Cu junction. We can also get arrays of the metal clusters upon breaking off of the junctions as shown in the inset of Figure 2b, and such clusters can be removed by applying a certain positive potential.^{36,43} Only one set of values for molecular junction conductance was observed, which indicates likely that there exists a dominant geometry between electrode and anchoring group in our experiment. However the possibility that many different bonding geometries with similar conductance give rise to the single broad peak in the histogram feature cannot be excluded either.

Figure 3 shows the representative conductance curves and histogram for malonic acid contacting to the Ag electrode. The potential was controlled at -5 mV and 45 mV vs Ag wire for the tip and the substrate, respectively. The histogram shows a pronounced peak located at 32 nS, which is lower than malonic acid binding to the Cu electrode. Also the order of conductance value is the same as that of succinic acid binding to the Cu and Ag electrodes.³⁶ It is explained by the difference in electronic coupling efficiency between the anchoring group and electrode as previously reported,^{33,36} which would change the contact conductance and thus influence the single molecule con-

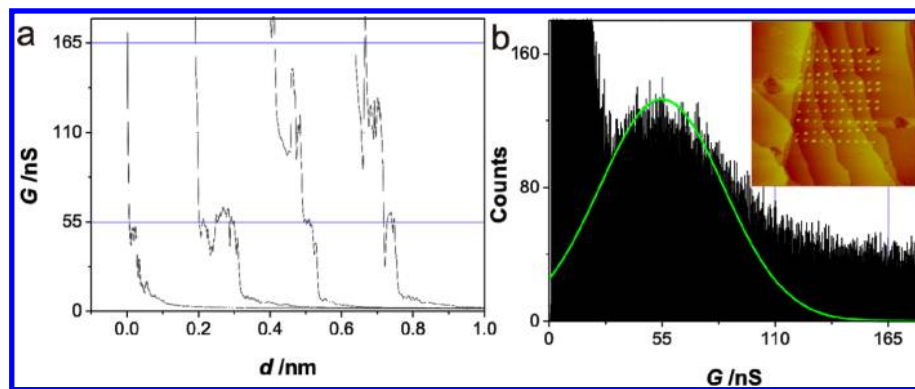


Figure 2. (a) Typical conductance traces and (b) conductance histogram of single molecule junction of Cu-malonic acid-Cu. The STM image ($200 \times 200 \text{ nm}^2$) of a 10×10 array of Cu clusters simultaneously generated with the conductance curves is shown in the inset of panel b.

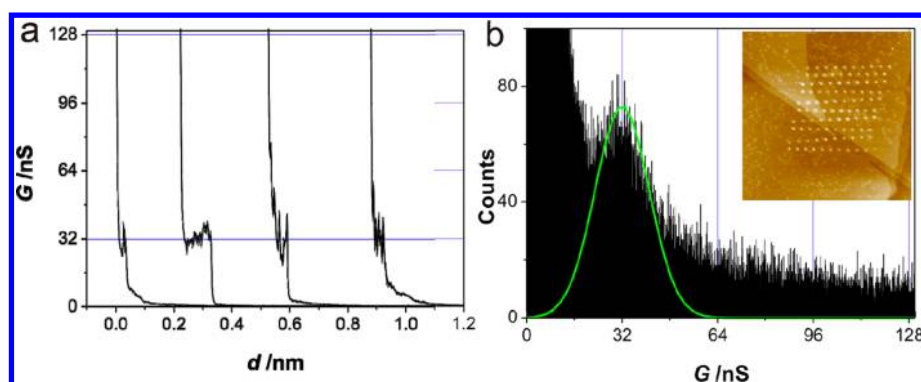


Figure 3. (a) Typical conductance traces and (b) conductance histogram of single molecule junction of Ag–malonic acid–Ag. The STM image ($200 \times 200 \text{ nm}^2$) of a 10×10 array of Cu clusters simultaneously generated with the conductance curves is shown in the inset of panel b. Solution: 1 mM Ag_2SO_4 + 1 mM malonic acid + 50 mM Na_2SO_4 .

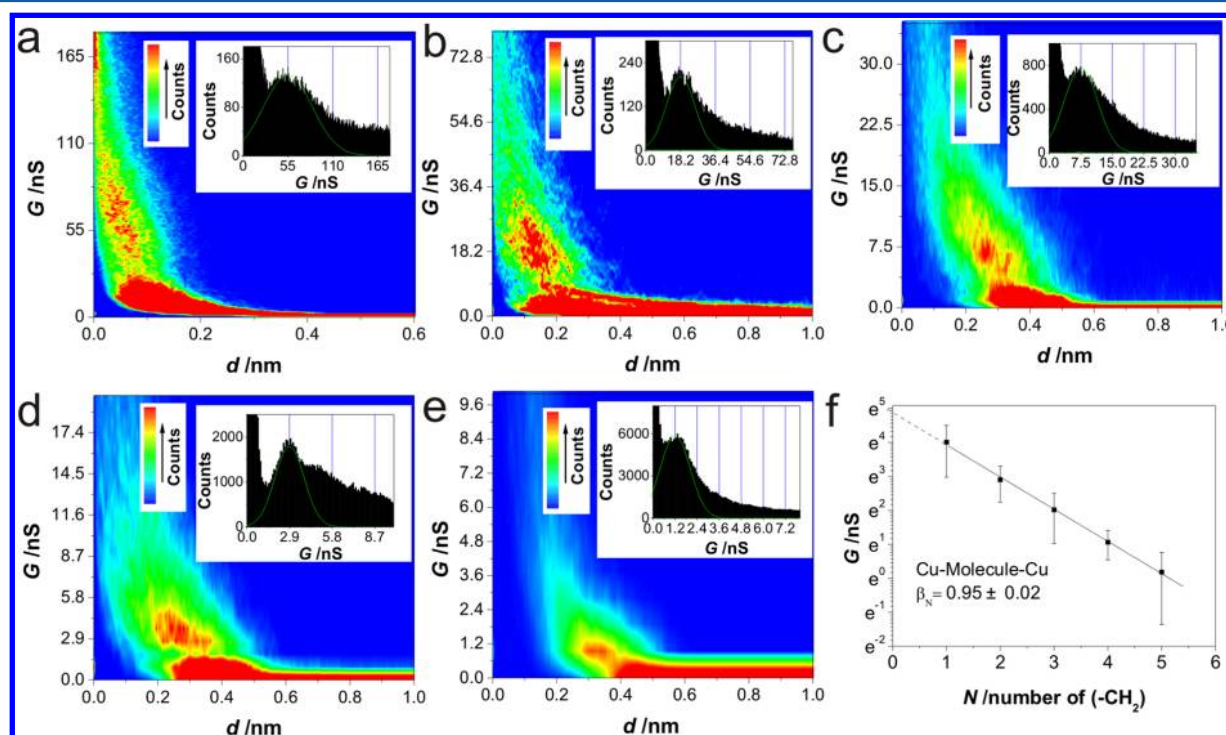


Figure 4. Two-dimensional histograms of single molecule conductance with contact of Cu for $\text{HOOC}-(\text{CH}_2)_n-\text{COOH}$ with $n =$ (a) 1, (b) 2, (c) 3, (d) 4, (e) 5. Insets are the corresponding conductance histograms. (f) Natural logarithmic plots of single-molecule conductance vs. number of $(-\text{CH}_2)$ units for molecular junctions formed with Cu electrodes.

ductance. Actually, the single molecule conductance is also determined by the energy coupling between the Fermi level of the electrode and the frontier molecular orbital level, and the conjugation of the molecular backbone.¹⁴ The former may be altered by change of the Fermi level of the electrode for a specified molecule to pursue energy level alignment.^{5,47,48} Those factors may be caused by the different conductance order for the molecule contact to the different metals, which will be discussed in the next section.

Length Dependence of Conductance. To investigate the conductance dependence on the molecular length with Cu and Ag electrodes, we measured the conductance of homologous series molecules of $\text{HOOC}-(\text{CH}_2)_n-\text{COOH}$ ($n = 1-5$). All experimental parameters are similar to the conductance measurement of malonic acid except the replacement of the target molecule.

Two-dimensional (2D) histogram is a statistical presentation of measured conductance as a function of stretching distance.⁴⁹⁻⁵¹ Briefly, a 2D histogram is realized by counting the number of data at each conductance value with each stretching distance out of hundreds or thousands of curves, and the origin of the stretching distance can be defined by that at a specified conductance value. Here we also present 2D histograms for the conductance of alkanedicarboxylic acid binding to the Cu electrode as shown in Figure 4a–e, while Ag electrode is shown in Figure 5a–e. Those conductance values are the same as the data treated with the traditional one-dimensional (1D) histogram method as shown in insets of Figures 4 and 5. Table 1 summarizes single molecule conductance with contact of Cu and Ag electrodes. Typically, the single molecular junction conductance decreases with the increasing of the molecular length for both Cu and Ag electrodes. The conductance of succinic acid binding to the Cu

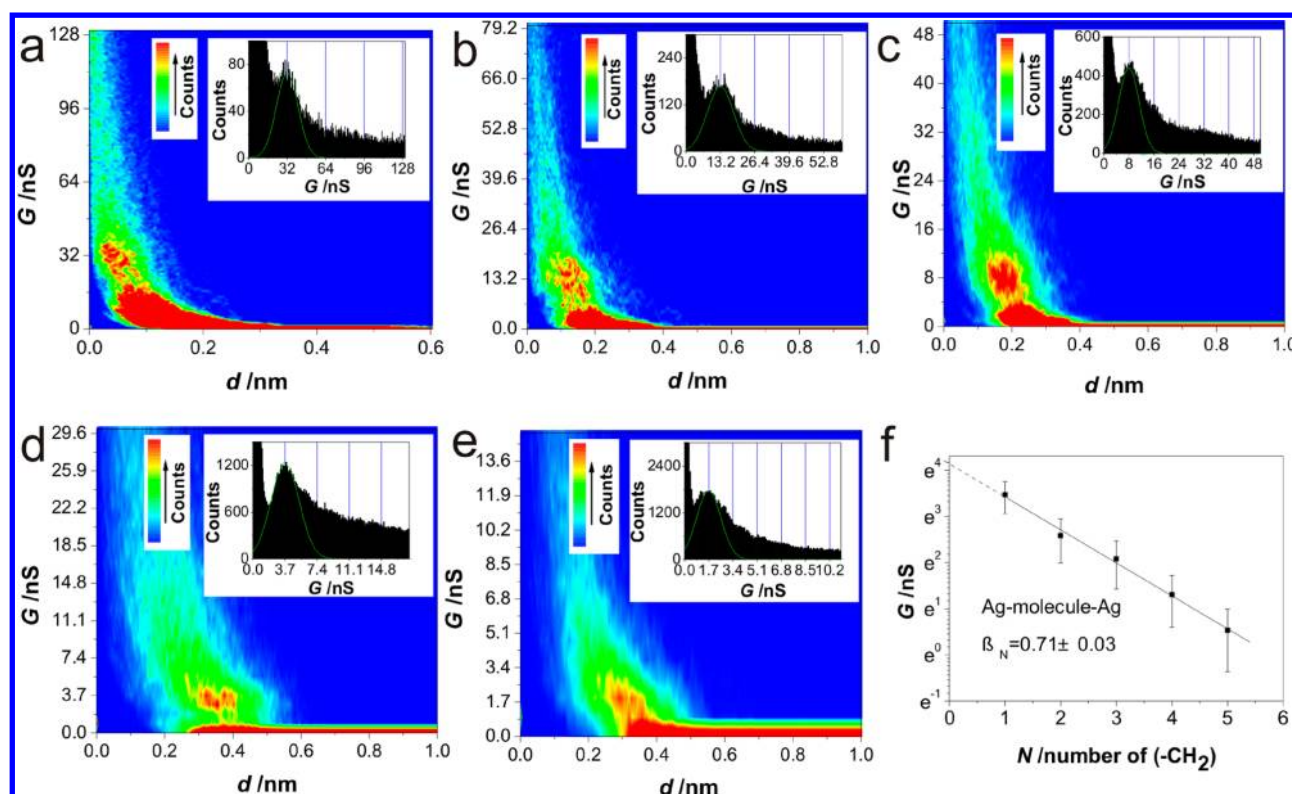


Figure 5. Two-dimensional histograms of single molecule conductance with contact of Ag for HOOC-(CH₂)_n-COOH with *n* = (a) 1, (b) 2, (c) 3, (d) 4, (e) 5. Insets are the corresponding conductance histograms. (f) Natural logarithmic plots of single-molecule conductance vs number of (-CH₂) units for molecular junctions formed with Ag electrodes.

Table 1. Summary of Single Molecule Conductance (nS) with Contact of Cu and Ag Electrodes

Cu-HOOC-(CH ₂) _n -COOH	<i>n</i>	Ag-HOOC-(CH ₂) _n -COOH
55	1	32
18.2	2	13.2
7.5	3	8.0
2.9	4	3.7
1.2	5	1.7

and Ag is consistent with our previous report,³⁶ which proves the reliability of the approach.

Superexchange mechanism is predicted for molecule junctions with saturated alkane chain (such as alkanedicarboxylic acid), and the conductance decreased exponentially with molecular length. At low bias, the conductance can be expressed as

$$G = G_{n=0} \exp(-\beta_N N)$$

where *G* is the molecular conductance, *N* is the number of methylene units, *G*_{*n*=0} is a constant determined by the molecule-electrode coupling strength and corresponds to the contact conductance, and β_{*N*} is the tunneling decay constant which describes the efficiency of electron transport along the molecules.

Regarding the current symmetric metal-molecule-metal junctions, β_{*N*} can be simply given by^{14,27,52}

$$\beta_N = 2\sqrt{\frac{2m\Phi}{\hbar^2}} d_0$$

m is the effective electron mass, and Φ is the barrier height indicating the energy between the Fermi level in the junction

and the molecular energy levels.^{14,33,52} ħ is the reduced Planck's constant. *d*₀ is the unit length of the alkane chain. Hence the β_{*N*} is decided by the alignment of the molecular energy levels relative to the Fermi energy level of the electrodes from the expression. Usually, β_{*N*} values of 0.8–1.1 per methylene unit are reported for saturated alkane binding to the Au, Pd, and Pt electrode,^{22,33} while the β_{*N*} values for molecular junctions binding to Cu and Ag electrodes are seldom reported.

Figure 4f and Figure 5f show natural logarithmic plots of single-molecule conductance vs number of (-CH₂) units for molecular junctions formed with Cu and Ag electrodes, respectively. The β_{*N*} is 0.95 ± 0.02 per (-CH₂) unit for Cu electrode, and 0.71 ± 0.03 for Ag electrode. These values are comparable with those reported in the literature for saturated alkane terminated with -COOH contact with Au,^{22,53} which is about 0.78 per (-CH₂) unit.

Clearly, the dependence of β_{*N*} on the different metal electrodes can be expected from the above equation. The small difference in the β_{*N*} for Cu and Ag electrodes is indeed observed, which might be explained by the different barrier height Φ in molecular junctions caused by the different of the *E*_{Fermi} of Cu and Ag electrode. Conversely, Ko et al. reported that the β_{*N*} values of α,ω-alkanes with headgroups of -SH and -NCS contacting Au, Pd, and Pt electrodes are almost the same by using STM-BJ, which gives β_{*N*} of about 1 per -CH₂.³³ Frisbie and co-workers found that β_{*N*} is 1.1 ± 0.1 for alkanedithiols and alkanethiols binding to Ag, Au, and Pt by using AFM,⁵² almost the same value of β_{*N*} for different metal electrodes. One of the proposed reasons is that the Fermi level is pinned with the energy positions of molecular states, and then the Φ is approximately the same for different metal contacts due to the bond dipole.^{34,52} It is worth mentioning

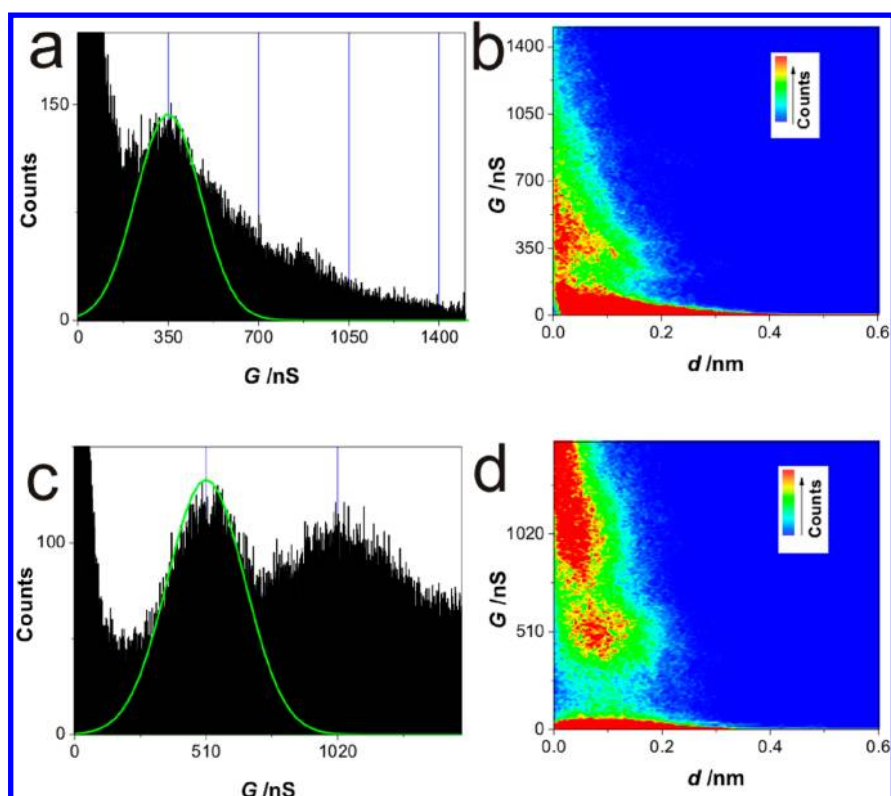


Figure 6. Conductance histogram of single molecule junction of (a) Cu–oxalic acid–Cu and (c) Ag–oxalic acid–Ag. Two-dimensional histograms of (b) Cu–oxalic acid–Cu and (d) Ag–oxalic acid–Ag showing single molecule junction as a function of STM tip-sample distance.

that those experiments were carried out in atmospheric environment or nonconductive organic solutions. In contrast, in the present work, the conductance of molecular junctions was measured with the potential control of electrodes, which may invalidate the pinning of the Fermi level to the energy positions of molecular states. The distinction of experimental parameter may cause the small difference in the metal dependence of the β . Additionally, Fatemi et al. found that the conductance of a molecular junction can be changed by the adsorption of the molecule onto metal binding sites which shifts the metal contact work function,⁵⁴ and this factor may also need to be taken into account. However, complete understanding of different β for Cu and Ag needs further theoretical and experimental investigations.

Contact Conductance of Molecular Junction. Contact conductance of the two anchoring groups ($G_{n=0}$) can be derived by plotting the single molecule conductance values against the number of methylene units of the molecules. The contact conductance for carboxylate group ($-\text{COO}^-$) binding to Cu and Ag electrodes is 132 nS and 63 nS as shown in Figures 4f and 5f, respectively. The dependence is attributed to the difference in electronic coupling efficiency between the anchoring group and electrodes. Typically, the chemisorbed contacts have higher contact conductance than physisorbed contacts.⁵² Interestingly, Frisbie and co-workers found that the contact conductance exhibits strong work function dependence and increases with the increasing metal work function for the thiol–metal contact, and the dependence was explained in terms of the metal–S bond dipoles.^{34,52,55} Similarly, our result is following the work function dependence in accordance with literature values of metal work function for Cu (4.65 eV) and Ag (4.26 eV).⁵⁶

We also observed the reversal of the conductance order with Cu and Ag electrodes at $n = 3$. For the molecules with $n = 3-5$, the single molecule conductance with Cu electrode is lower than that with Ag, as opposed to the case of molecules with $n = 1, 2$, due to the larger values of both β_N and $G_{n=0}$ for Cu than Ag electrodes.

Conductance of Molecule with Ultrashort Chain.

Conductance measurement of single molecule junctions is mainly based on molecules with a long chain. There are seldom reports on the molecular conductance with ultrashort chain except ethanedithiol molecule bridging to Au electrode.⁵⁷ But this kind of molecule would be useful when small resistance is needed, and the study of conductance of molecule will also help to understand the electron transport mechanism through ultrashort distance between two electrodes.

To investigate the conductance mechanism of the ultrashort molecule, oxalic acid was used as the target molecule. The conductance of the Cu–oxalic acid junction is 350 nS, while the Ag–oxalic acid junction is 510 nS as shown in Figure 6. By using $G = G_{n=0} \exp(-\beta_N N)$, and assuming that this molecular length dependence of the conductance can be extrapolated to short length, the conductance of Cu–oxalic acid and Ag–oxalic acid is 132 nS and 63 nS from Figures 4f and 5f, respectively. Clearly, these values are lower than the experimental results.

What is the reason for the difference conductance between the experiment and extrapolated value from the length dependence of conductance? First, the better π -electron conjugation of the short oxalic acid should be considered. We have performed DFT code SIESTA^{35,58} calculation about the HOMO and LUMO levels for alkanedicarboxylic acids ($(\text{HOOC}-(\text{CH}_2)_n-\text{COOH}, n = 0-5)$ without metal electrodes. The oxalic acid has a small HOMO–LUMO gap (3.6 eV) compared with the other longer molecule with about 5.1 eV.

Second, “through-bond” (TB) and “through-space” (TS) mechanisms have been supposed for the current transport in molecular junctions.¹⁴ The current flows through the bond of the molecule in TB, while the current flows through the gap between the two electrodes in TS. The conductance of a molecule can be divided into two components as follows:

$$G = G_{\text{TB}} + G_{\text{TS}}$$

where G_{TB} and G_{TS} give the efficiency of current transport through the TB and TS mechanism. TB is the commonly dominant mechanism when the molecules are chemically bonded at both ends and not very short. The molecules' ($\text{HOOC}-(\text{CH}_2)_n-\text{COOH}$, $n = 1-5$) conductance mainly facilitates current flow in the TB mechanism, with the β_{N} about 0.95 ± 0.02 and 0.73 ± 0.04 per $(-\text{CH}_2)$ unit for Cu and Ag electrodes, respectively. For an ultrashort molecule, such as oxalic acid with molecular length about 0.49 nm, the TS should also be included for the current transport, for the tunneling current (I) would become very large at such an electrode distance.

Here we consider that for very short molecules G_{TS} , originating from the tunneling current between tip and substrate, might become dominant with respect to the G_{TB} . Assuming the extrapolated contact conductance of $G_{n=0,\text{Cu}} = 132$ nS and $G_{n=0,\text{Ag}} = 63$ nS at $n = 0$ may be regarded as $G_{\text{TB,Cu}}$ and $G_{\text{TB,Ag}}$ of oxalic acid, the corresponding $G_{\text{TS,Cu}}$ would be 218 nS and $G_{\text{TS,Ag}}$ 447 nS according to the above formula. It should be mentioned that, because of the better π -electron conjugation of the short oxalic acid than that of the long chain carboxylic acids at $n = 0$, the actual G_{TB} of the oxalic acid would be larger than the extrapolated values, leading to smaller G_{TS} for both Cu and Ag electrodes.

The difference between $G_{\text{TS,Cu}}$ and $G_{\text{TS,Ag}}$ can be explained by the tunneling current between tip and sample:^{59,60}

$$I \propto V_{\text{b}} \rho_{\text{s}}(0, E_{\text{F}}) \exp(-A \Phi_{\text{eff}}^{1/2} s)$$

V_{b} is the bias voltage, $\rho_{\text{s}}(0, E_{\text{F}})$ is the local density of states at Fermi level, A is constant, Φ_{eff} is the effective tunnel barrier, and s is the tip-sample distance. For V_{b} , A , and s the same for both electrodes, the different tunneling current is caused by the different effective tunneling barriers and local density of states between the Cu and Ag electrode. The result shows that the TS mechanism should be considered when the molecular length is very short or the distance between two electrodes is short.⁶¹

CONCLUSIONS

We have systematically investigated alkanedicarboxylic acid ($\text{HOOC}-(\text{CH}_2)_n-\text{COOH}$, $n = 1-5$) binding to the Cu and Ag electrodes by the ECSTM-BJ approach. The results show the molecular length dependence of conductance, giving β_{N} of 0.95 ± 0.02 per $(-\text{CH}_2)$ unit for Cu electrode and 0.71 ± 0.03 for Ag electrode, which is decided by the alignment of the molecular energy levels relative to the Fermi energy level of the electrodes. Meanwhile contact conductance determined by the electronic coupling efficiency between the anchoring group and metal electrodes shows the order $G_{n=0,\text{Cu}} > G_{n=0,\text{Ag}}$. Reversal of the conductance order for Cu and Ag electrodes for the series of carboxylic acid molecules is observed. For the molecules with $n = 3-5$, the single molecule conductance with Cu electrode is lower than that with Ag, opposite to the case for molecules with $n = 1, 2$. In addition, we measured the ultrashort molecule junctions using oxalic acid, through which the TS mechanism

should also be considered besides the TB mechanism when the distance between the two electrodes is very short. The present work shows that electronic coupling efficiency between the anchoring group and electrodes plays an important role in the molecular conductance and contact conductance, also the tunneling decay constant can be influenced by the different electrodes.

AUTHOR INFORMATION

Corresponding Author

*X.-S.Z.: tel, +86 579 82286876; fax, +86 579 82282595; e-mail, xszhou@zjnu.edu.cn. B.-W.M.: tel, +86 592 2186979; fax, +86 592 2183047; e-mail, bwmao@xmu.edu.cn.

Notes

The authors declare no competing financial interest.

ACKNOWLEDGMENTS

We gratefully acknowledge the financial support by NSFC (No. 21003110, 21273204, 20973141, and 20911130235), the Planned Science and Technology Project of Zhejiang Province (No. 2011C37052), and the Scientific Research Fund of Zhejiang Provincial Education Department (No. Y201016469).

REFERENCES

- (1) Song, H.; Kim, Y.; Jang, Y. H.; Jeong, H.; Reed, M. A.; Lee, T. *Nature* **2009**, *462*, 1039–1043.
- (2) Diez-Perez, I.; Li, Z.; Hihath, J.; Li, J.; Zhang, C.; Yang, X.; Zang, L.; Dai, Y.; Feng, X.; Muellen, K.; Tao, N. *Nat. Commun.* **2010**, *1*, 31.
- (3) Xu, B. Q.; Xiao, X. Y.; Yang, X. M.; Zang, L.; Tao, N. J. *J. Am. Chem. Soc.* **2005**, *127*, 2386–2387.
- (4) Li, C.; Mishchenko, A.; Li, Z.; Pobelov, I.; Wandlowski, T.; Wurthner, F.; Bagrets, A.; Evers, F. *J. Phys.: Condens. Matter* **2008**, *20*, 374122.
- (5) Zhou, X. S.; Liu, L.; Fortgang, P.; Lefevre, A. S.; Serra-Muns, A.; Raouafi, N.; Amatore, C.; Mao, B. W.; Maisonhaute, E.; Schöllhorn, B. *J. Am. Chem. Soc.* **2011**, *133*, 7509–7516.
- (6) McCreery, R.; Dieringer, J.; Solak, A. O.; Snyder, B.; Nowak, A. M.; McGovern, W. R.; DuVall, S. *J. Am. Chem. Soc.* **2003**, *125*, 10748–10758.
- (7) Metzger, R. M. *Acc. Chem. Res.* **1999**, *32*, 950–957.
- (8) Chen, J.; Reed, M. A.; Rawlett, A. M.; Tour, J. M. *Science* **1999**, *286*, 1550–1552.
- (9) Xiao, X. Y.; Nagahara, L. A.; Rawlett, A. M.; Tao, N. J. *J. Am. Chem. Soc.* **2005**, *127*, 9235–9240.
- (10) Chen, F.; He, J.; Nuckolls, C.; Roberts, T.; Klare, J. E.; Lindsay, S. *Nano Lett.* **2005**, *5*, 503–506.
- (11) Xu, B. Q.; Tao, N. J. *Science* **2003**, *301*, 1221–1223.
- (12) Zhou, X. S.; Chen, Z. B.; Liu, S. H.; Jin, S.; Liu, L.; Zhang, H. M.; Xie, Z. X.; Jiang, Y. B.; Mao, B. W. *J. Phys. Chem. C* **2008**, *112*, 3935–3940.
- (13) Venkataraman, L.; Klare, J. E.; Nuckolls, C.; Hybertsen, M. S.; Steigerwald, M. L. *Nature* **2006**, *442*, 904–907.
- (14) Salomon, A.; Cahen, D.; Lindsay, S.; Tomfohr, J.; Engelkes, V. B.; Frisbie, C. D. *Adv. Mater.* **2003**, *15*, 1881–1890.
- (15) Chen, F.; Hihath, J.; Huang, Z. F.; Li, X. L.; Tao, N. J. *Annu. Rev. Phys. Chem.* **2007**, *58*, 535–564.
- (16) Heath, J. R. *Annu. Rev. Mater. Res.* **2009**, *39*, 1–23.
- (17) McCreery, R. L.; Bergren, A. J. *Adv. Mater.* **2009**, *21*, 4303–4322.
- (18) Song, H.; Reed, M. A.; Lee, T. *Adv. Mater.* **2011**, *23*, 1583–1608.
- (19) Lu, Q.; Liu, K.; Zhang, H. M.; Du, Z. B.; Wang, X. H.; Wang, F. S. *ACS Nano* **2009**, *3*, 3861–3868.
- (20) Liu, H. M.; Wang, N.; Zhao, J. W.; Guo, Y.; Yin, X.; Boey, F. Y. C.; Zhang, H. *ChemPhysChem* **2008**, *9*, 1416–1424.

- (21) Bruot, C.; Hihath, J.; Tao, N. J. *Nat. Nanotechnol.* **2012**, *7*, 35–40.
- (22) Chen, F.; Li, X. L.; Hihath, J.; Huang, Z. F.; Tao, N. J. *J. Am. Chem. Soc.* **2006**, *128*, 15874–15881.
- (23) Luo, L.; Choi, S. H.; Frisbie, C. D. *Chem. Mater.* **2010**, *23*, 631–645.
- (24) Tao, N. J. *Nat. Nanotechnol.* **2006**, *1*, 173–181.
- (25) Schull, G.; Frederiksen, T.; Arnau, A.; Sanchez-Portal, D.; Berndt, R. *Nat. Nanotechnol.* **2011**, *6*, 23–27.
- (26) Li, X. L.; He, J.; Hihath, J.; Xu, B. Q.; Lindsay, S. M.; Tao, N. J. *J. Am. Chem. Soc.* **2006**, *128*, 2135–2141.
- (27) Li, C.; Pobelov, I.; Wandlowski, T.; Bagrets, A.; Arnold, A.; Evers, F. J. *Am. Chem. Soc.* **2008**, *130*, 318–326.
- (28) Hu, Y. B.; Zhu, Y.; Gao, H. J.; Guo, H. *Phys. Rev. Lett.* **2005**, *95*, 156803.
- (29) Boardman, B. M.; Widawsky, J. R.; Park, Y. S.; Schenck, C. L.; Venkataraman, L.; Steigerwald, M. L.; Nuckolls, C. *J. Am. Chem. Soc.* **2011**, *133*, 8455–8457.
- (30) Ballesteros, L. M.; Martin, S.; Momblona, C.; Marques-Gonzalez, S.; Lopez, M. C.; Nichols, R. J.; Low, P. J.; Cea, P. *J. Phys. Chem. C* **2012**, *116*, 9142–9150.
- (31) Hong, W.; Manrique, D. Z.; Moreno-García, P.; Gulcur, M.; Mishchenko, A.; Lambert, C. J.; Bryce, M. R.; Wandlowski, T. *J. Am. Chem. Soc.* **2012**, *134*, 2292–2304.
- (32) Kiguchi, M.; Miura, S.; Takahashi, T.; Hara, K.; Sawamura, M.; Murakoshi, K. *J. Phys. Chem. C* **2008**, *112*, 13349–13352.
- (33) Ko, C. H.; Huang, M. J.; Fu, M. D.; Chen, C. H. *J. Am. Chem. Soc.* **2010**, *132*, 756–764.
- (34) Kim, B.; Choi, S. H.; Zhu, X. Y.; Frisbie, C. D. *J. Am. Chem. Soc.* **2011**, *133*, 19864–19877.
- (35) Bai, M. L.; Liang, J. H.; Xie, L. Q.; Sanvito, S.; Mao, B. W.; Hou, S. M. *J. Chem. Phys.* **2012**, *136*, 104701.
- (36) Zhou, X. S.; Liang, J. H.; Chen, Z. B.; Mao, B. W. *Electrochem. Commun.* **2011**, *13*, 407–410.
- (37) Chen, F.; Huang, Z. F.; Tao, N. J. *Appl. Phys. Lett.* **2007**, *91*, 162106.
- (38) Kiguchi, M. *Appl. Phys. Lett.* **2009**, *95*, 073301.
- (39) Kiguchi, M.; Miura, S.; Hara, K.; Sawamura, M.; Murakoshi, K. *Appl. Phys. Lett.* **2007**, *91*, 053110.
- (40) Kolb, D. M.; Ullmann, R.; Will, T. *Science* **1997**, *275*, 1097–1099.
- (41) Wei, Y. M.; Zhou, X. S.; Wang, J. G.; Tang, J.; Mao, B. W.; Kolb, D. M. *Small* **2008**, *4*, 1355–1358.
- (42) Wang, J. G.; Tang, J.; Fu, Y. C.; Wei, Y. M.; Chen, Z. B.; Mao, B. W. *Electrochem. Commun.* **2007**, *9*, 633–638.
- (43) Zhou, X. S.; Wei, Y. M.; Liu, L.; Chen, Z. B.; Tang, J.; Mao, B. W. *J. Am. Chem. Soc.* **2008**, *130*, 13228–13230.
- (44) Kim, Y.; Cho, K.; Lee, K.; Choo, J.; Gong, M.-s.; Joo, S.-W. *J. Mol. Struct.* **2008**, *878*, 155–161.
- (45) Han, S. W.; Joo, S. W.; Ha, T. H.; Kim, Y.; Kim, K. *J. Phys. Chem. B* **2000**, *104*, 11987–11995.
- (46) Payer, D.; Comisso, A.; Dmitriev, A.; Strunskus, T.; Lin, N.; Wöll, C.; DeVita, A.; Barth, J.; Kern, K. *Chem.—Eur. J.* **2007**, *13*, 3900–3906.
- (47) Li, X. L.; Hihath, J.; Chen, F.; Masuda, T.; Zang, L.; Tao, N. J. *J. Am. Chem. Soc.* **2007**, *129*, 11535–11542.
- (48) Li, X. L.; Xu, B. Q.; Xiao, X. Y.; Yang, X. M.; Zang, L.; Tao, N. J. *Faraday Discuss.* **2006**, *131*, 111–120.
- (49) Martin, C. A.; Ding, D.; Sorensen, J. K.; Bjornholm, T.; van Ruitenbeek, J. M.; van der Zant, H. S. J. *J. Am. Chem. Soc.* **2008**, *130*, 13198–13199.
- (50) Schneebeli, S. T.; Kamenetska, M.; Cheng, Z.; Skouta, R.; Friesner, R. A.; Venkataraman, L.; Breslow, R. *J. Am. Chem. Soc.* **2011**, *133*, 2136–2139.
- (51) Kamenetska, M.; Koentopp, M.; Whalley, A. C.; Park, Y. S.; Steigerwald, M. L.; Nuckolls, C.; Hybertsen, M. S.; Venkataraman, L. *Phys. Rev. Lett.* **2009**, *102*, 126803–126804.
- (52) Engelkes, V. B.; Beebe, J. M.; Frisbie, C. D. *J. Am. Chem. Soc.* **2004**, *126*, 14287–14296.
- (53) Martin, S.; Haiss, W.; Higgins, S.; Cea, P.; Lopez, M. C.; Nichols, R. J. *J. Phys. Chem. C* **2008**, *112*, 3941–3948.
- (54) Fatemi, V.; Kamenetska, M.; Neaton, J. B.; Venkataraman, L. *Nano Lett.* **2011**, *11*, 1988–1992.
- (55) Beebe, J. M.; Engelkes, V. B.; Miller, L. L.; Frisbie, C. D. *J. Am. Chem. Soc.* **2002**, *124*, 11268–11269.
- (56) Michaelson, H. B. *J. Appl. Phys.* **1977**, *48*, 4729–4733.
- (57) Kiguchi, M.; Sekiguchi, N.; Murakoshi, K. *J. Phys. Conf. Ser.* **2008**, *100*, 052059.
- (58) Soler, J. M.; Artacho, E.; Gale, J. D.; García, A.; Junquera, J.; Ordejón, P.; Sánchez-Portal, D. *J. Phys.: Condens. Matter* **2002**, *14*, 2745.
- (59) Tersoff, J.; Hamann, D. R. *Phys. Rev. Lett.* **1983**, *50*, 1998–2001.
- (60) Halbritter, J.; Repphun, G.; Vinzelberg, S.; Staikov, G.; Lorenz, W. J. *Electrochim. Acta* **1995**, *40*, 1385–1394.
- (61) Gotsmann, B.; Riel, H.; Lortscher, E. *Phys. Rev. B* **2011**, *84*, 205408.